



ELSEVIER

## Development of a very large area microstrip gas chamber for the CMS central tracking system

F. Angelini <sup>a</sup>, R. Bellazzini <sup>a,\*</sup>, M. Bozzo <sup>b</sup>, A. Brez <sup>a</sup>, M.M. Massai <sup>a</sup>, R. Raffo <sup>a</sup>,  
G. Spandre <sup>a</sup>, M. Spezziga <sup>a</sup>, A. Toropin <sup>c</sup>

<sup>a</sup> INFN-Pisa and University of Pisa, Pisa, Italy

<sup>b</sup> INFN-Genova and University of Genova, Genova, Italy

<sup>c</sup> INR-Academy of Sciences, Moscow, Russian Federation

### Abstract

A very large area microstrip gas chamber ( $250 \times 100 \text{ mm}^2$ ), thought to be the building block of the CMS barrel tracker, has been built and undergone extensive tests with X-ray sources and particle beams. Rate capability, uniformity of response along the strip and charging-up effect for different gas gain and bias schemes have been measured in laboratory. A systematic study on the long-term stability of its performance (ageing) at high rates has been carried out both with standard and “clean” mechanical assemblies. Stability measurements under high voltage were performed. Studies of spatial resolution and efficiency for minimum ionizing particles were carried out with different gas gap, gas mixture, angle of incidence and avalanche gain.

### 1. Introduction

Despite of the success of the high energy physics experiments and of the predictions of the Standard Model, many fundamental questions of the elementary particle world, as the origin of the particle masses and the hierarchy of generations of quarks and leptons, are still waiting to be answered.

The next significant step towards a better understanding of the laws of nature is expected from the study of particle interactions at the LHC energy. To detect signatures of new physics it is necessary to identify and precisely measure muons, electrons and photons as it has been emphasised in the design of CMS, one of the two general purpose detectors for LHC.

Primary goal of CMS is to reconstruct in highly congested event topologies and with high momentum precision all high  $p_T$  muons and isolated electrons produced in the central rapidity region. The pattern recognition at the luminosity of LHC represents therefore the main problem to be solved.

A tracking detector with high granularity and precision is thus required with the consequence that the number of

electronics channels hugely increase ( $\approx 10^7$ ). Furthermore the severe environmental conditions of CMS, i.e. high radiation level and very high magnetic field, pose a great challenge in the design of the inner tracking detector.

For the good performance obtained even in experimental conditions close to those described above, the microstrip gas chamber has shown to meet the CMS requirements and, for this reason, it has been chosen as one of the constituent parts of the CMS central tracking system [1,2].

To reduce the number of channels necessary to cover large volumes, hence the cost of the tracker while maintaining a cell occupancy level around 1%, a very large area ( $25 \times 10 \text{ cm}^2$ ) MSGC has been built.

The detector has been realized with a substrate made of cheap, industrial, glass which is only slightly affected by charging-up problems. The substrate is very thin ( $300 \mu\text{m}$ ) to minimize multiple scattering and photon conversion probability.

The long term stability of the detector when it is exposed to high rate of ionizing radiation has been extensively studied. Preliminary stability measurements under high voltage have also been performed.

Using X-ray sources or, according to the case, minimum ionizing particle beams all the main parameters of this detector, i.e. rate capability, uniformity of response along the strip, spatial resolution and efficiency have been studied with different gas mixture, avalanche gain, gas gap and angle of incidence of the radiation.

\* Corresponding author. Tel +39 50 880271, fax +39 50 880317, e-mail bellazzini@pisa.infn.it.

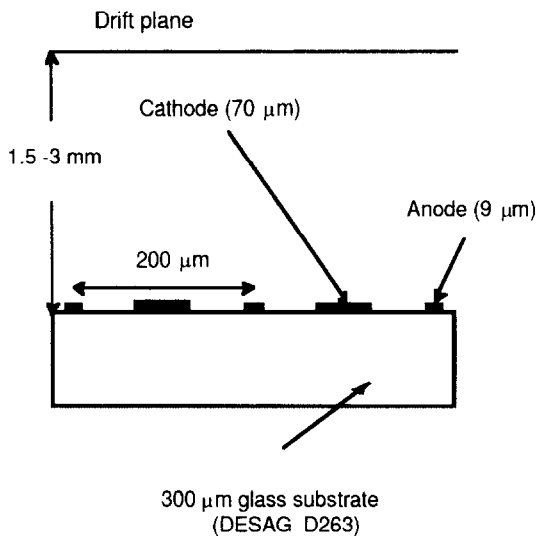


Fig. 1. A cross section of the detector.

The behaviour of the MSGC in strong magnetic field (up to 2.3 T) and the possibility to fully compensate the effect of the  $E \times B$  factor on the degradation of the spatial resolution, at least for high  $p_T$  tracks, has been also accurately studied and reported in a previous paper [3].

## 2. The detector

A cross section of the detector internal structure is shown in Fig. 1.

The strip's width and pitch are almost standard, while what is really new in this prototype is the very large active

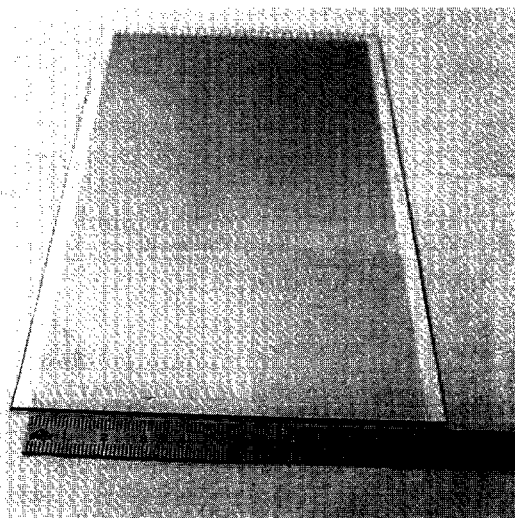


Fig. 2. A photograph of the very large MSGC.



Fig. 3. A photograph of the optimized layout of the strip edges.

area ( $250 \times 100 \text{ mm}^2$ ) obtained on a thin substrate ( $300 \mu\text{m}$ ).

Fig. 2 is a photograph of how the detector looks like.

Fig. 3 shows the rounded shape given to the strip ends to avoid sparking effects at the edges where the electric field reinforces.

For ageing studies two kinds of detectors were produced. They differed in the metal, aluminum or gold, used for the strips and were assembled alternatively using standard (fiberglass, nylon, araldite, ...) and "clean" (glass, quartz, stainless steel) materials.

## 3. Laboratory tests

### 3.1. Charging, uniformity, rate capability

The choice of the substrate is an important element for a stable operation of the detector. In particular, sufficiently low surface resistivity materials are preferred to avoid, even at low radiation fluxes, the so-called charging-up [4,5], i.e. a time and flux dependent modification of the gain. This effect is due to a local variation of the electric field caused by the accumulation on the surface of positive ions produced in the avalanche process.

The glass used here is DESAG 263, an industrial, cheap, glass with ionic conductivity ( $\approx 10^{15} \Omega \text{ cm}$ ) but with rather low content of sodium ions ( $\approx 5\%$ ).

To study the time dependence of the gain at short-term, the detector, whose aluminum strips were engraved with a lift-off technique, has been irradiated with an X-ray source at a rate of  $10^4 \text{ photons/mm}^2$ . This radiation rate is approximately what is expected in the innermost part of the CMS barrel.

The signal current has been recorded with a Keithley 487 picoammeter for a period of nearly 3 minutes. A 10% gain drop has been observed only during the first few seconds of exposure as it is shown in Fig. 4.

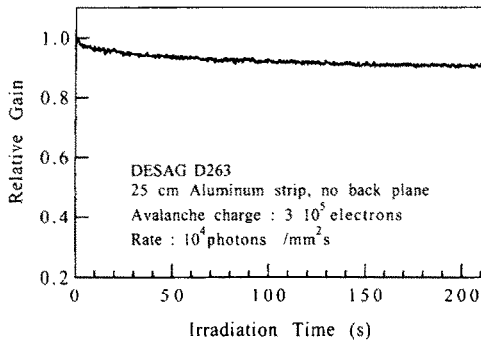


Fig. 4. Short-term measurement of the gain stability.

Besides the electrical properties of the substrate, the other factor which largely determines the charging-up effects is represented by the bias scheme of the back and drift plane.

As Fig. 5 shows, a further significant decrease in gain is observed when the back electrode is referred to the cathode potential instead of the anode one, even if slightly higher gain can be obtained in this configuration.

In the case  $V_{back} = V_{cathode}$ , in fact, a larger number of field lines end on the substrate thus increasing the density of negative surface charge which is proportional to the normal component of the electric field [6].

Fig. 6 shows the normal component of the field as computed with the electrostatic modeler ELECTRO [7] for the three different bias schemes: a)  $V_{back} = V_{anode}$ , b)  $V_{back} = V_{cathode}$ , c) no back.

In case  $V_{back} = V_{anode}$  the vertical component of the electric field is negative, i.e. enters the substrate only up to a distance of  $\sim 13 \mu\text{m}$  from the anode.

With  $V_{back} = V_{cathode}$  the electric field at the anode is stronger and enters the substrate for a much longer distance,  $40 \mu\text{m}$ , while the configuration with no back represents the intermediate case.

A decrease of 10% in the gain has been measured in different bias conditions by Bohm et al. [8].

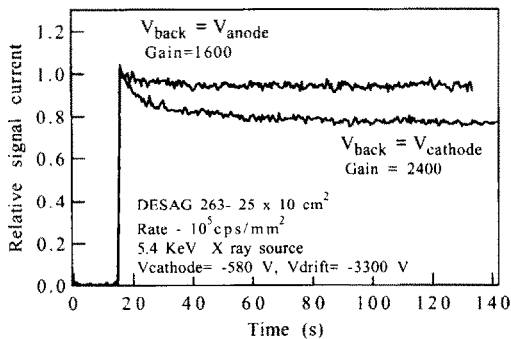


Fig. 5. Time dependence of the gain for the two different bias schemes.

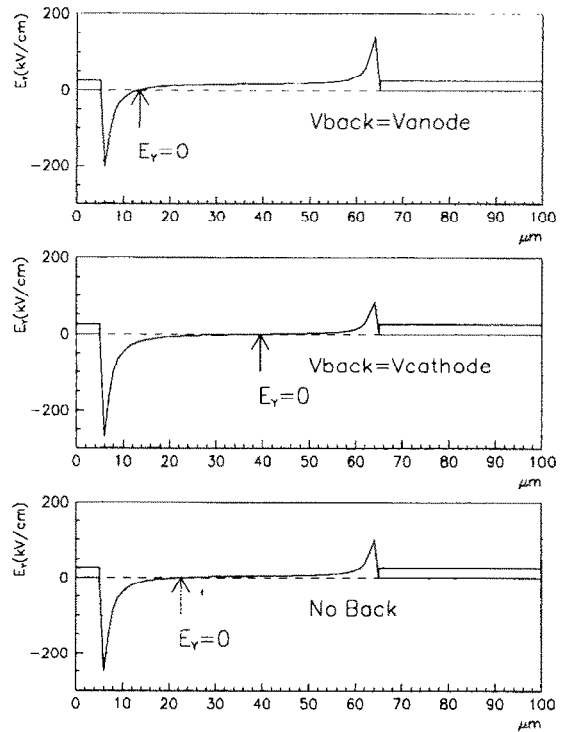


Fig. 6. The vertical component of electric field on the substrate for the bias schemes:  $V_{back} = V_{anode}$ ,  $V_{back} = V_{cathode}$ , no back.

As shown in Figs. 7a and 7b there is also a dependence of charging with the gain which is 10% maximum in the least favourable bias condition  $V_{back} = V_{cathode}$ .

Another important feature for detectors of such size is the uniformity of response along the strip.

This measurement has been performed by recording both the average signal amplitude and the mean charge coming from a detector with strips made of aluminum,  $1 \mu\text{m}$  thick (Fig. 8). A variation less than 4% has been measured in both cases.

Fig. 9 shows the rate capability measured with this detector. The total avalanche charge was  $3 \times 10^5$  electrons and the drift field was  $8 \text{ kV/cm}$ . No significant variation in pulse height has been observed for fluxes ranging from 10 to  $100 \text{ kHz/mm}^2$  corresponding to the anticipated particle rates for MSGCs in CMS.

### 3.2. Ageing

For the MSGCs to be used in the radiation environment of LHC, the most critical issue is ageing, namely the deterioration of the detector response arising from long-term exposure to high charged particles fluxes.

Detectors assembled with standard components, e.g. fiberglass, glues and nylon tubing, and flushed with stan-

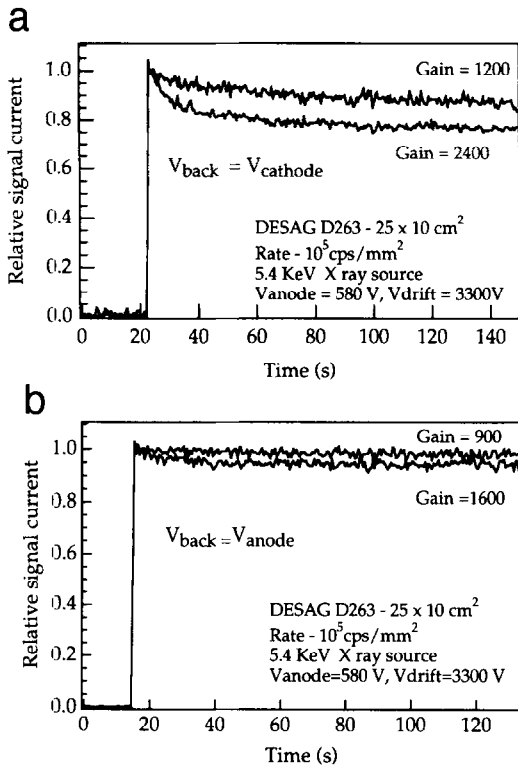


Fig. 7. (a) Dependence of charging with gain in the case  $V_{back} = V_{cathode}$ . (b) Dependence of charging with gain in the case  $V_{back} = V_{anode}$ .

ard, not purified, gases, undergo fast and irreversible degradation of the response. To avoid, or at least to reduce, the ageing process some chambers have been assembled using components made only of glass and metal (quartz spacers and metal plated glass windows). Furthermore, ultra-high vacuum, non-outgassing, glue (Torr-seal) have been applied throughout. The gas system has been also significantly improved, using mass-flow meters and

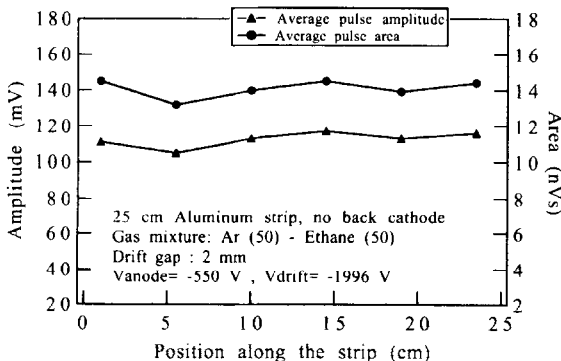


Fig. 8. Uniformity of response along the 25 cm strip.

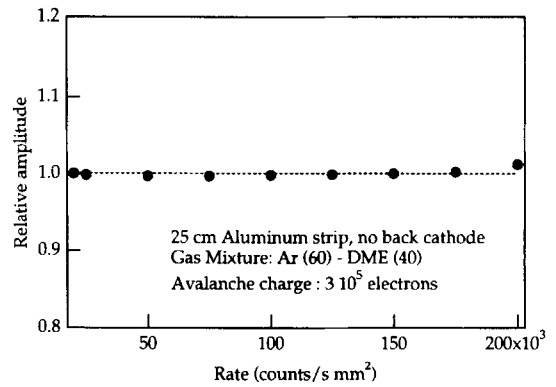


Fig. 9. Rate capability.

stainless steel tubing even for the inlet and outlet of the chamber.

The best results were obtained with a detector with gold plated strips and an aluminized glass drift cathode.

It was illuminated with a 5.4 keV X-ray source producing an avalanche charge of  $5 \times 10^5$  electrons in Ar–DME gas mixture (60–40).

With a flux of  $1 \text{ MHz/mm}^2$  the observed variation in gain was  $-0.15\%$  per  $\text{mC/cm}$  and the integrated charge reached was  $60 \text{ mC/cm}$  corresponding to  $\geq 10$  years of equivalent LHC operation at  $r = 1 \text{ m}$  (Fig. 10).

No loss of gain up to  $160 \text{ mC/cm}$  of strip have been independently reported by the RD28 collaboration using a similar set-up [9].

It must be pointed out that, though a “very clean” assembling and a high purified gas system largely contribute to increase the lifetime of the detector, the factor that more strongly influences the ageing is, by our experience, the metalization material of the strips.

At this purpose a comparative study has been carried out on two kinds of detectors: one with strips made of aluminum and the other one with gold strips, the rest being identical. From this study it has resulted that chambers

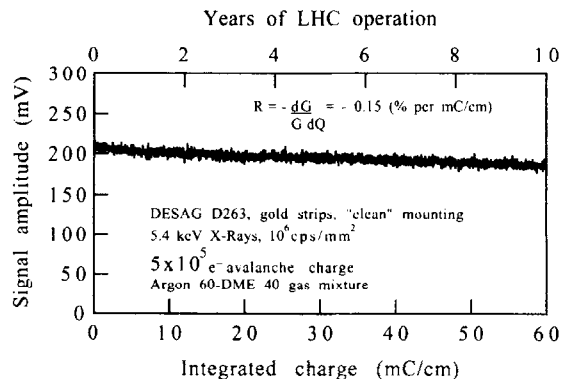


Fig. 10. Very long-term measurement of the gain stability (ageing).

with gold strips are much less affected by ageing (but are also a little less robust) respect to detectors made with aluminum strips. This probably is due to the fact that gold, being quite inert, is not attacked chemically by reactions with species produced during the avalanche process.

Parallel to the study of survivability at high dose of radiation the stability of response under high voltage has also been studied. It has been indeed pointed out that a continuous power supply could cause permanent modification in the electrical and structural properties of the sub-

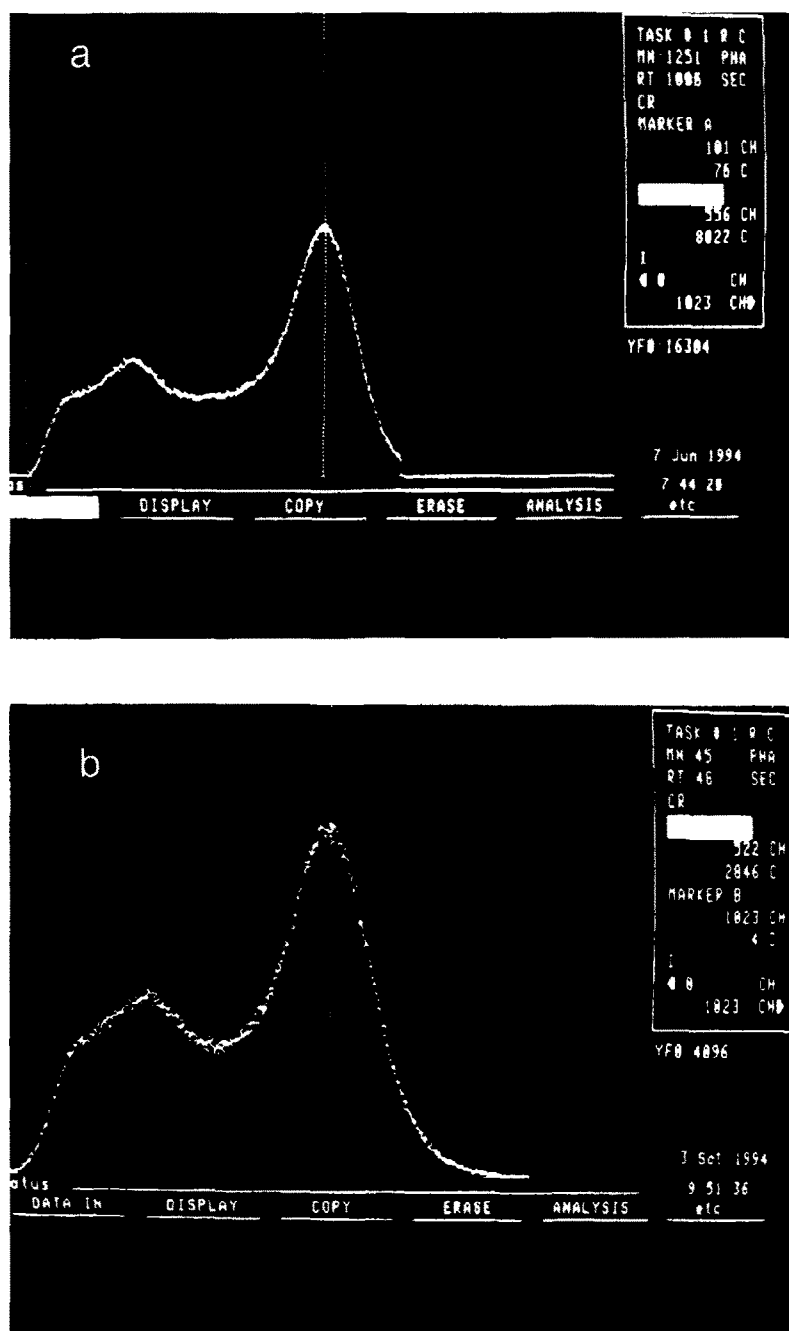


Fig. 11. (a)  $^{55}\text{Fe}$  pulse height distribution at the beginning of the stability measurement under HV.  $V_{\text{cathode}} = -570$  V,  $V_{\text{drift}} = -3000$  V. (b)  $^{55}\text{Fe}$  pulse height distribution recorded 3 months after that one of (a).

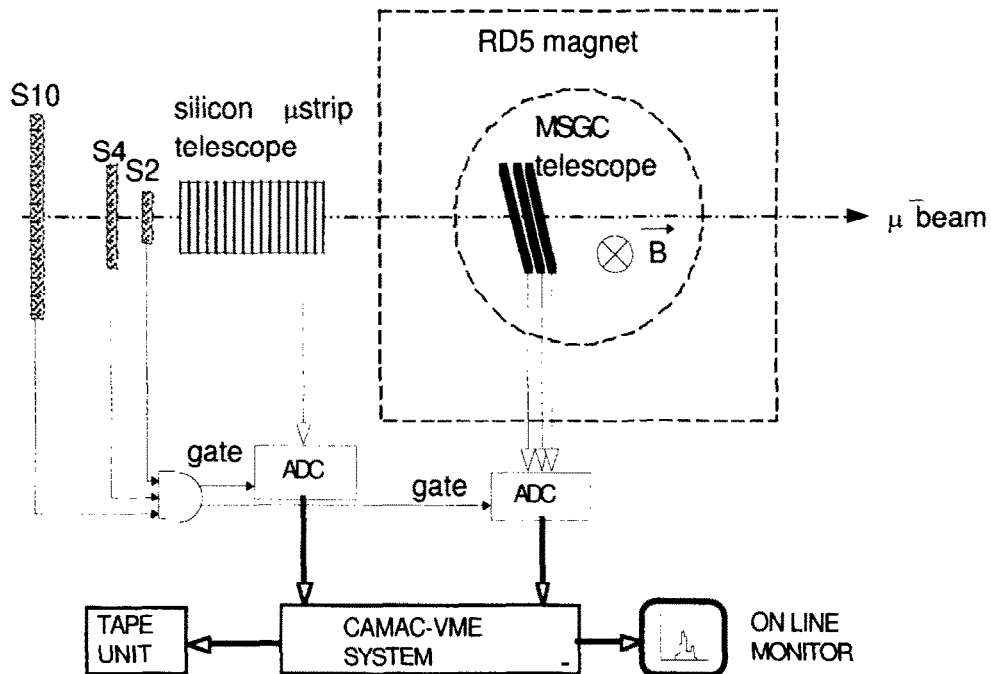


Fig. 12. The general view of the experimental set-up.

strate due to migration of the ions along the electric field lines.

For this reason a MSGC with aluminum strips has been, and still is, continuously supplied with HV, and, only from time to time, a pulse height distribution of an  $^{55}\text{Fe}$  source is recorded. During a period of 4 months no significant variation in the distribution shape has been observed.

Figs. 11a and 11b show two pulse height spectra, from three anode strips, taken at a 3 months time lag.

#### 4. Particle beam tests

##### 4.1. Experimental set-up

The study of the MSGC spatial resolution and efficiency for minimum ionizing particles has been performed at the CERN SPS with a  $225 \text{ GeV}/c \mu^-$  beam.

Different gas gap, gas mixture, avalanche gain and angle of track incidence were used.

A telescope of two  $25 \times 10 \text{ cm}^2$  MSGC's, with 1.6 and 2.9 mm gas gap respectively, and one MGC was installed in the H2/RD5 beam line. A silicon microstrip telescope was used as external position reference system.

The three chambers were mounted on special supports which could rotate with respect to an axis parallel to the strips and orthogonal to the beam direction. A schematic view of the experimental set-up is shown in Fig. 12.

During the test run several gas mixtures were used (pure DME, argon–DME, DME– $\text{CO}_2$  and DME– $\text{CF}_4$ ).

These gas mixtures were chosen for their high ionization density, fast drift velocity and small diffusion coefficient, factors which should provide high resolution and full detection efficiency in the thin detectors which have to be used at LHC.

##### 4.2. Spatial resolution

The read-out chain was a fast and low noise hybrid preamplifier mounted on the detector board, followed by a

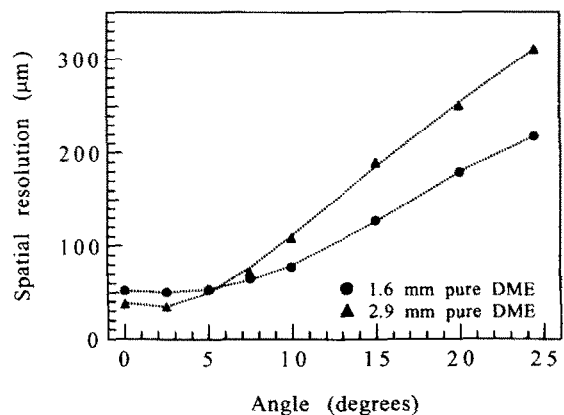


Fig. 13. The dependence of the spatial resolution on the incidence angle of the track for two gas gaps.

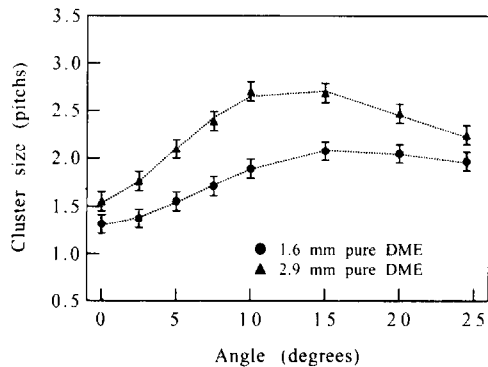


Fig. 14. The dependence of the cluster size on the track angle.

remote shaping amplifier (Laben 5185). The delta current response of the shaping amplifier was adjusted to have 10 ns rise-time and 50 ns width (FWHM).

The anode signals were recorded individually by means of a 12 bit ADC (LeCroy 2282), while the cathode signals were read-out in groups of sixteen.

For each chamber a simple cluster algorithm allowed to determine the charge cluster produced by the particle, whose coordinate was then computed with the center of gravity method.

The spatial resolution was then estimated from the rms width of the distribution of the track residuals.

Fig. 13 shows the dependence of the spatial resolution as a function of the incidence angle of the track, for the two MSGCs with 1.6 (chamber 1) and 2.9 (chamber 2) mm gap.

The figure refers to a gas filling of pure DME and a gas gain of roughly 2000 ( $HV_{\text{cathode1,2}} = -700$  V,  $HV_{\text{drift1}} = -2100$  V,  $HV_{\text{drift2}} = 3400$  V). The spatial resolution of the thicker chamber comes out to be the best up to an angle of nearly  $5^\circ$ .

At large angle the thinner chamber performs much better because the parallax error starts to affect strongly the track reconstruction.

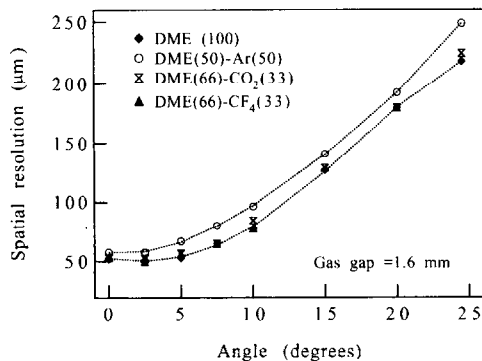


Fig. 15. The dependence of the spatial resolution on the incidence angle of the track for different gas mixtures.

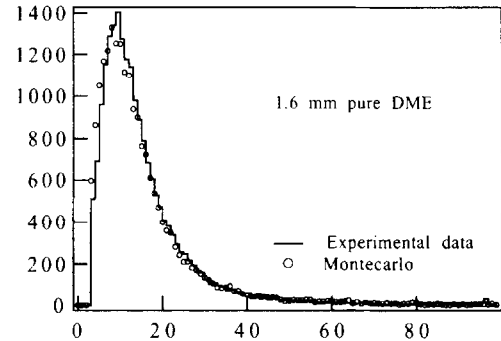


Fig. 16. The pulse height distribution obtained with 1.6 mm pure DME.

Fig. 14 shows the dependence of the cluster size on the track angle obtained, for the two MSGCs, in the same experimental conditions of Fig. 13.

Fig. 15 shows the spatial resolution, as a function of the track angle, obtained with: pure DME, DME- $\text{CO}_2$ , DME- $\text{CF}_4$ , DME-Ar. The data refers to the detector with the gap of 1.6 mm.

Ar (50)-DME (50) is clearly the poorest mixture, while no significant variation is observed for the three mixtures at higher content of DME.

#### 4.3. Detection efficiency

Two typical Landau distributions, obtained with 1.6 and 2.9 mm pure DME, are shown in Figs. 16 and 17 respectively, at  $0^\circ$  incidence angle.

A Monte-Carlo prediction is superimposed on the same figures.

The close matching between experimental and simulated data demonstrates the validity of the Monte-Carlo model, we have developed, to simulate the dynamic processes of charge transport and collection (ionization, diffusion and multiplication) which take place inside the detector.

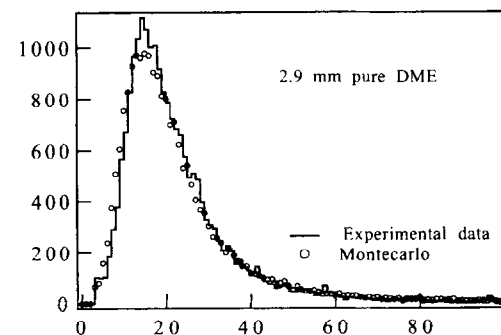


Fig. 17. The same as Fig. 16 but with 2.9 mm pure DME.

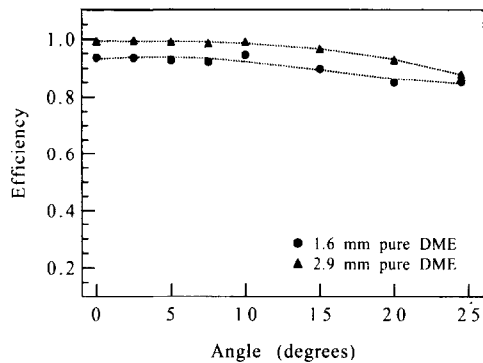


Fig. 18. The cluster detection efficiency in pure DME for 1.6 and 2.9 mm gas gap.

As it appears clearly from Fig. 16 a high cluster detection efficiency (> 95%) for mips is obtained also for the extremely thin chamber.

The cluster detection efficiency as a function of the track angle, for both gas thicknesses, is reported in Fig. 18. The figure refers to a pure DME filling.

Data, obtained with the thinner detector, for different gas mixtures, are compared in Fig. 19.

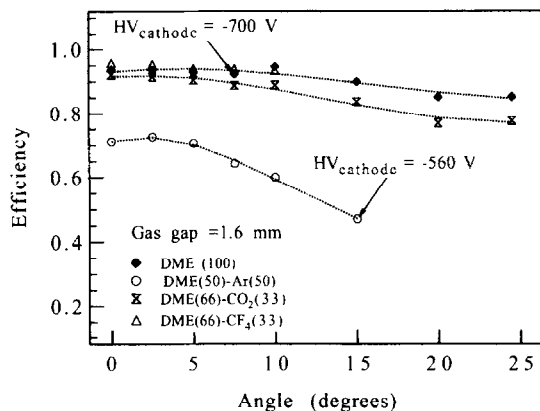


Fig. 19. The detection efficiency for different gas mixtures (gas gap = 1.6 mm).

## 5. Conclusions

The operating characteristics in various configurations of the very large area MSGC have been thoroughly investigated under laboratory and test beam conditions. The detector matches well the stringent requirements of CMS as concerns:

- dimensions, which minimize costs without compromising pattern recognition,
- radiation length, which fits into the material budget of the central tracker,
- stability of gain at high radiation flux and over extended period,
- behaviour in presence of intense magnetic field,
- high detection efficiency and spatial resolution even for very small gas thickness.

For all these reasons this detector is being considered a reasonable baseline solution for the CMS central tracker.

## Acknowledgements

We want to express our gratitude to all the RD5 team for their hospitality and help.

We thank G. Decarolis, M. Favati, C. Magazzu and S. Tolaini of INFN-Pisa and A. Morelli of INFN-Genova for their enthusiastic technical support.

## References

- [1] CMS Collaboration, Letter of Intent, CERN/LHCC 92-3.
- [2] CMS Collaboration, Status Report and Milestones CERN/LHCC 94-20.
- [3] F. Angelini et al., Nucl. Instr. and Meth. A 343 (1994) 441.
- [4] R. Bouclier et al., CERN-PPE/93-04.
- [5] J.E. Bateman and J.F. Connolly, RAL-92-085.
- [6] R. Bellazzini and M.A. Spezziga, INFN PI/AE 03-94.
- [7] ELECTRO - I.E.S., Manitoba, Canada.
- [8] J. Bohm et al., CERN PPE/94-115.
- [9] L. Alunni et al., Nucl. Instr. and Meth. A 348 (1994) 109.